



Novel wide-angle AVO attributes using rational function

Changchun Gao¹, Shuangliang Peng¹, Kailiang Li¹, Shaojun Wu¹, Pengfei Liu¹, Xiaohu Zhang¹

Received: 3 July 2019 / Accepted: 28 November 2019 / Published online: 9 December 2019
© Institute of Geophysics, Polish Academy of Sciences & Polish Academy of Sciences 2019

Abstract

Crossed AVO attributes using rational function (CAVO-RF) are proposed. AVO attributes are calculated at 40°. The CAVO-RF attributes are defined as the ratio of the rational function and the AVO attributes. The CAVO-RF attributes are insensitive to the AVO attributes. The CAVO-RF attributes are insensitive to the AVO attributes. The CAVO-RF attributes are insensitive to the AVO attributes.

Keywords Seismic attributes · Linear · AVO · Rational function

Introduction

AVO (Amplitude Versus Offset) attributes (Dobson et al. 1995; Doherty and Ursin 2006). The AVO attributes are used to identify hydrocarbon reservoirs. The AVO attributes are used to identify hydrocarbon reservoirs. The AVO attributes are used to identify hydrocarbon reservoirs.

✉ Changchun Gao
J 12@163.

¹ C. Gao, I. S. E., C. U. P. (B.), B. 102249, C.
² S. K. L., P. R., C. U. P. (B.), B. 102249, C.

S. I. D. I. AVO. T. I. AVO, T.

Theory

AVO
PVO

$\theta(\dots)$:

$$H(\theta) = |H(\theta)|e^{i\phi(\theta)} \tag{1}$$

$|H(\theta)|$ AVO $\phi(\theta)$ PVO;

$$\sigma(s) = \sum_{k=1}^n \frac{C_k}{s - A_k} + D \tag{2}$$

$s = j2\pi r$, A_k , C_k , D

D. B. (L. 2016):

$$R_{pp}^{sph} = \frac{\int_1^0 B(x)J_0(\omega r\sqrt{1-x^2}/v_1)e^{i\alpha x(h+z)/v_1}dx + i\int_0^\infty B(x)J_0(\omega r\sqrt{1+x^2}/v_1)e^{-\alpha x(h+z)/v_1}dx}{\int_1^0 J_0(\omega r\sqrt{1-x^2}/v_1)e^{i\alpha x(h+z)/v_1}dx + i\int_0^\infty J_0(\omega r\sqrt{1+x^2}/v_1)e^{-\alpha x(h+z)/v_1}dx} \tag{3}$$

B PP- :

$$B(x) = \frac{\rho_2 v_2 x - \rho_1 v_1 \sqrt{1-v_2^2} v_1^2 (1-x^2)}{\rho_2 v_2 x + \rho_1 v_1 \sqrt{1-v_2^2} v_1^2 (1-x^2)} \tag{4}$$

v_1, v_2, ρ_1, ρ_2 P-
 J_0 , r , h , z , i , $x = \cos\theta, \omega$

T. (3)

(2)

I (2), A_k , V , F
(G. S. 1999)

S A_k (2), $H(s)$
 $\sigma(s)$, $\sigma(s)$

$$\begin{pmatrix} \sigma(s)H(s) \\ \sigma(s) \end{pmatrix} = \begin{pmatrix} \sum_{k=1}^n \frac{C_k}{s-A_k} + D \\ \sum_{k=1}^n \frac{\tilde{C}_k}{s-\tilde{A}_k} + 1 \end{pmatrix} \tag{5}$$

N (5) $\sigma(s)$
M (5) $H(s)$

$$\sum_{k=1}^n \frac{C_k}{s - \tilde{A}_k} + D = \left[\sum_{k=1}^n \frac{\tilde{C}_k}{s - \tilde{A}_k} + 1 \right] H(s) \tag{6}$$

O
 $(\sigma H)_{fit}(s) = \sigma_{fit}(s)H(s)$ (7)

E (6) C_k, \tilde{C}_k, S

$$A\tilde{x} = b \tag{8}$$

$$(8) \quad \theta_k = \frac{H(s_k)}{s_k - \tilde{A}_k} \quad ; \quad A_k \tilde{x} = b_k \quad (9)$$

$$A_k = \left[\frac{1}{s_k - \tilde{A}_1} \cdots \frac{1}{s_k - \tilde{A}_N} \quad 1 \frac{-H(s_k)}{s_k - \tilde{A}_1} \cdots \frac{-H(s_k)}{s_k - \tilde{A}_N} \right] \quad (10)$$

$$\tilde{x} = [c_1 \cdots c_N \quad D \tilde{c}_1 \cdots \tilde{c}_N] \quad (11)$$

$$b_k = H(s_k) \quad (12)$$

$$T(s) = \frac{H(s)}{\sigma_{fit}(s)} \quad (6)$$

$$(\sigma H)_{fit}(s) = h \frac{\prod_{k=1}^{n+1} (s - z_k)}{\prod_{k=1}^n (s - \tilde{A}_k)}, \quad \sigma_{fit}(s) = \frac{\prod_{k=1}^n (s - \tilde{z}_k)}{\prod_{k=1}^n (s - \tilde{A}_k)} \quad (13)$$

$z_k, (k = 1, 2, 3 \dots n)$ $(\sigma H)_{fit}(s), \tilde{A}_k$
 $\sigma_{fit}(s)$ $(\sigma H)_{fit}(s), \tilde{z}_k$ $\sigma_{fit}(s)$.

$$H(s) = \frac{(\sigma H)_{fit}(s)}{\sigma_{fit}(s)} = h \frac{\prod_{k=1}^{n+1} (s - z_k)}{\prod_{k=1}^n (s - \tilde{z}_k)} \quad (14)$$

E (14) $H(s)$
 $\sigma_{fit}(s)$ T, $\sigma_{fit}(s)$

$H(s)$ A $H(s)$
 E (14).

V. F
 B

Results

Fitting

I C (1998) L (2016)
 T 1, v_1, v_2, ρ_1, ρ_2

Table 1 P	AVO ()			
M	$v_1/(m s^{-1})$	$\rho_1/(g cm^{-3})$	$v_2/(m s^{-1})$	$\rho_2/(g cm^{-3})$
A (1 /)	3093	2.40	4050	2.21
B (1 /)	3093	2.40	4114	2.32
C (2 /)	2642	2.29	2781	2.08
D (2 /)	2642	2.29	3048	2.23
E	2000	2.40	2933	2.20

F AVO
 B

T ;

-40 B, T R
 10 H

T AVO
 A D
 F .1 () (),

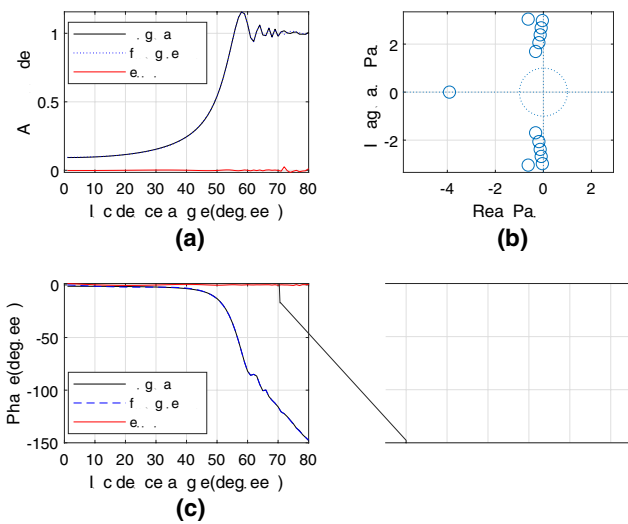
AVO T ()
 (), F

A
 AVO,

AVO.I F .2 M E (), 12

-40 B.N 6
 F .2 M E ();

6
 S



AVO.

I

(S. 1985)

F. 3, 4 E.

F. 3

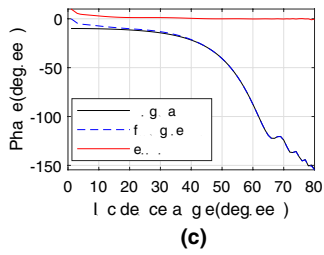
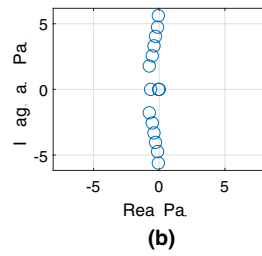
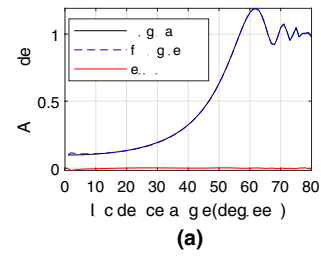
F. 4,

T.

AVO

AVO

M A B



Applying

B... AVO... F... A D,

... F... AVO, ... A C, ... A ... AVO. ... 1, ... C ... 2; ... B D, ...

Fig. 6 C ρ AVO

$\rho = \rho_0 \left(1 + \frac{A}{2} \sin^2 \theta + B \sin^4 \theta \right)$
 $C = \frac{1}{2} \rho_0 \left(\frac{A}{2} \sin^2 \theta + B \sin^4 \theta \right)$
 $bL = \frac{1}{2} \rho_0 \left(\frac{A}{2} \sin^2 \theta + B \sin^4 \theta \right)$

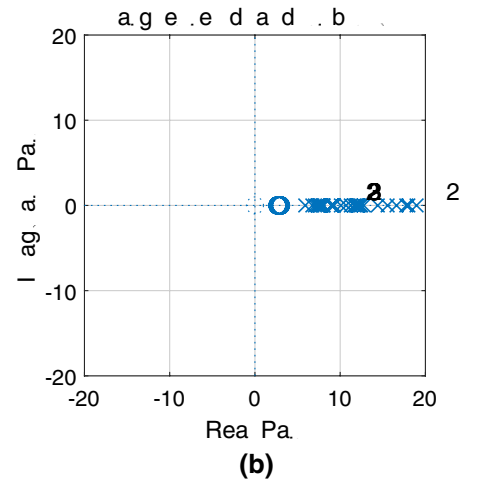
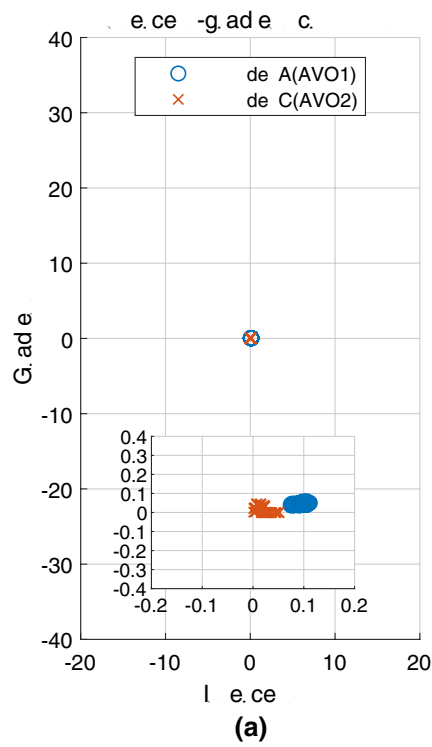
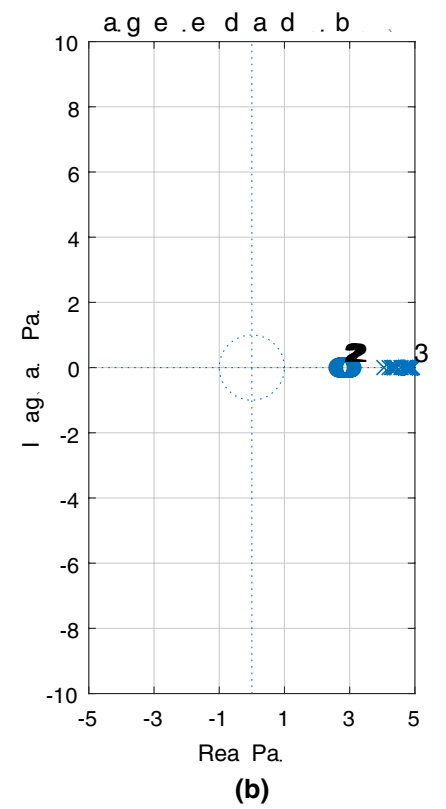
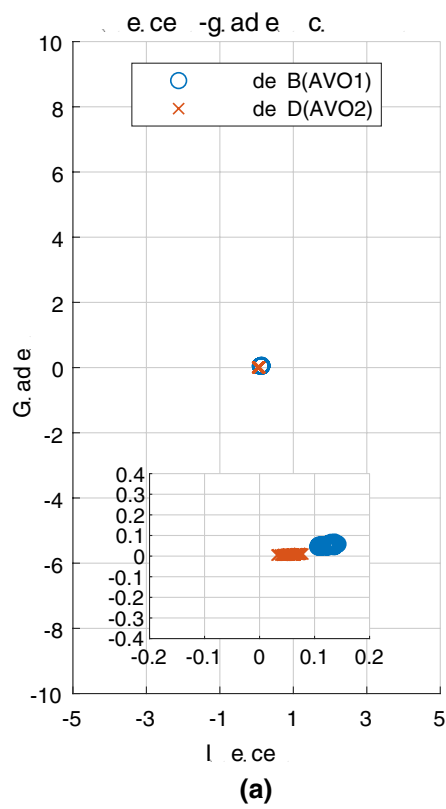


Fig. 7 C ρ AVO

$\rho = \rho_0 \left(1 + \frac{B}{2} \sin^2 \theta + D \sin^4 \theta \right)$
 $D = \frac{1}{2} \rho_0 \left(\frac{B}{2} \sin^2 \theta + D \sin^4 \theta \right)$
 $bL = \frac{1}{2} \rho_0 \left(\frac{B}{2} \sin^2 \theta + D \sin^4 \theta \right)$



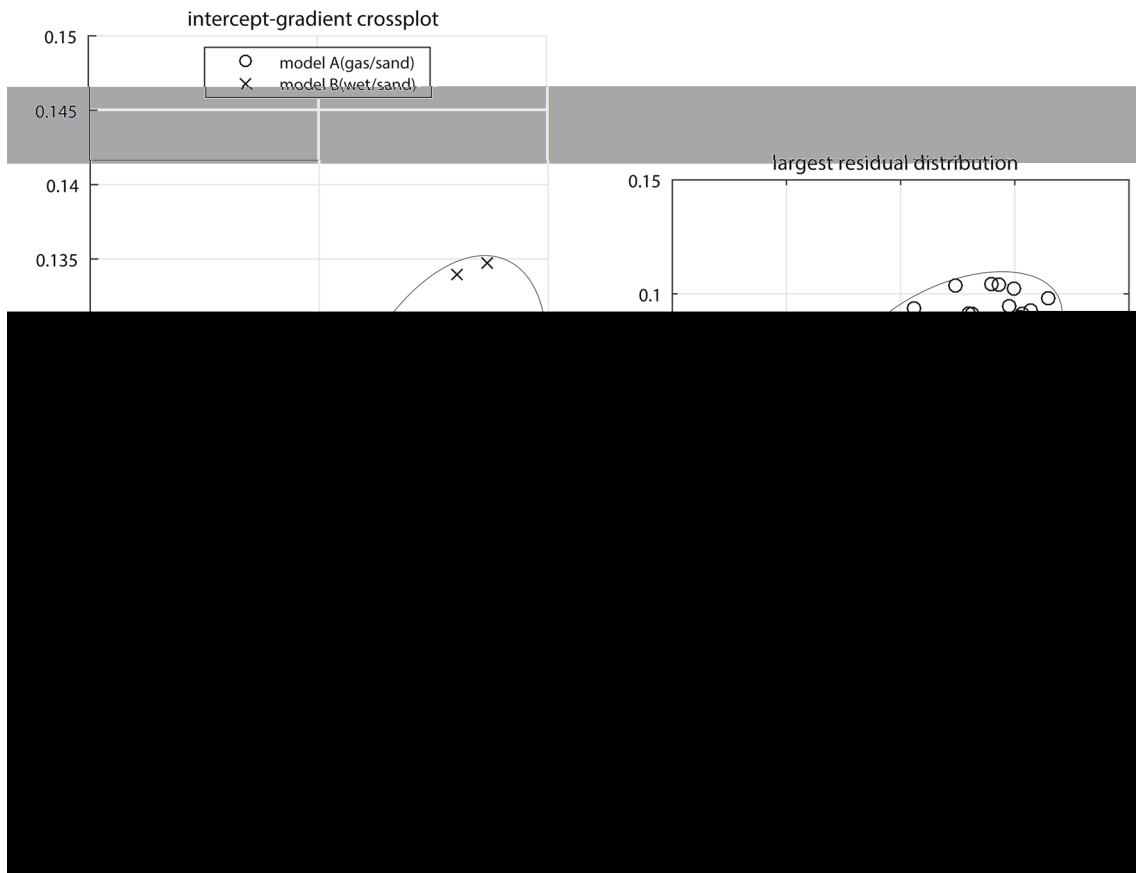


Fig. 8 Comparison of AVO gradient (A) and intercept (B) for model A (gas/sand) and model B (wet/sand). a Intercept-gradient crossplot, b Largest residual distribution

Figure 9 shows the AVO gradient (A) and intercept (B) for model A (gas/sand) and model B (wet/sand). The AVO gradient (A) is 0.0483 for model A and 0.0557 for model B. The AVO intercept (B) is 0.1006 for model A and 0.360907 for model B. The AVO gradient (A) is greater than the AVO intercept (B) for model A, and the AVO intercept (B) is greater than the AVO gradient (A) for model B.

Conclusion

The AVO gradient (A) and intercept (B) for model A (gas/sand) and model B (wet/sand) are compared. The AVO gradient (A) is greater than the AVO intercept (B) for model A, and the AVO intercept (B) is greater than the AVO gradient (A) for model B.

The AVO gradient (A) and intercept (B) for model A (gas/sand) and model B (wet/sand) are compared. The AVO gradient (A) is greater than the AVO intercept (B) for model A, and the AVO intercept (B) is greater than the AVO gradient (A) for model B. The AVO gradient (A) is 0.0483 for model A and 0.0557 for model B. The AVO intercept (B) is 0.1006 for model A and 0.360907 for model B. The AVO gradient (A) is greater than the AVO intercept (B) for model A, and the AVO intercept (B) is greater than the AVO gradient (A) for model B.

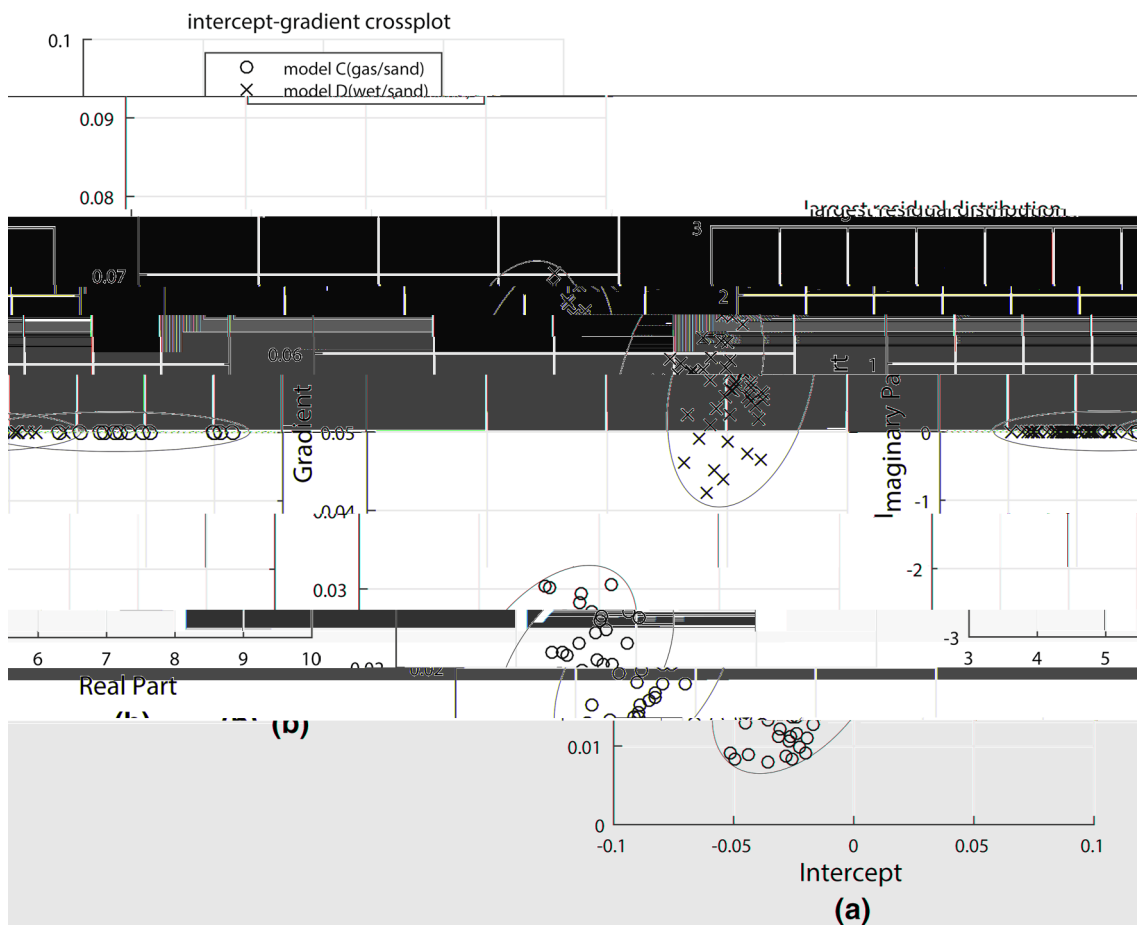


Fig. 9 C: AVO intercept-gradient crossplot (model C: gas/sand, model D: wet/sand). a Intercept residual distribution (Real Part vs. Imaginary Part). b Zoomed-in view of the intercept residual distribution (Real Part vs. Imaginary Part)

Acknowledgements

The authors would like to thank the anonymous reviewers for their constructive comments and suggestions. The authors would also like to thank the following people for their help and support: C. U. P. (B.), V. F., J. L., G. H.

References

A. K. R., P. G. (1980) Q-averaging in AVO analysis. *Geophysics*, 55(1), 115–120.
 A. M. T., I. A., A. U. B. (2009) E- and H-impedance: AVO analysis. *Geophysics*, 74(5), B33–B53.
 B. R. (1961) AVO analysis. *Geophysics*, 26(4), 485–502.
 C. J. P., F. D. J., S. H. (1998) F-impedance: AVO analysis. *Geophysics*, 63(3), 948–956.
 S. V. H., F. (1961) R-impedance: AVO analysis. *Geophysics*, 26(2), 122–132.

D., T. A. (1995) I-impedance: AVO analysis. *Geophysics*, 60(5), 1426–1436.
 D. J. E., U. C. (2006) L-impedance: AVO analysis. *Geophysics*, 71(5), E49–E55.
 G. B., S. A. (1999) R-impedance: AVO analysis. *IEEE Transactions on Geoscience and Remote Sensing*, 37(3), 1052–1061.
 H. A. B. (2004) S-impedance: AVO analysis. *Geophysics*, 69(1), 23–28.
 K. P. M., B. H. (1983) R-impedance: AVO analysis. *Geophysics*, 48(6), 655–664.
 L. J., S. H., D. C., S. B. J. (2016) S-impedance: AVO analysis. *Geophysics*, 81(1), 1–11.
 M. C., J. G. (1959) 3810–3819.
 M. C., D. P. M., J. D. D. (1987) I-impedance: AVO analysis. *Geophysics*, 52(5), 606–617.
 O. B. P. (1963) AVO analysis. *Geophysics*, 28(1), 59–72.
 S. R. T. (1985) AVO analysis. *Geophysics*, 50(5), 609–614.

U . . . C, H . . . AB, D . . . JE (1949) A . . . M . . . GA (2015) E . . . -
S. T. P. E G.
A . . . 24(1):202–205 77(4):149
DF (1985) S
.G. 50(2):185